Inorganic Chemistry

pubs.acs.org/IC
Article

Unusually Effective Blue-to-UVC Upconversion of Pr^{3+}-Doped $Sr_3Lu(PO_4)_3$ and $Ba_3Lu(PO_4)_3$ Phosphors: A Comparative Study

Nadiia Rebrova,* Alexander Grippa, Patrycja Zdeb-Stańczykowska, and Przemysław J. Dereń

Cite This: *Inorg. Chem.* 2025, 64, 11146−11154
Read Online

ABSTRACT: Many pathogens, including bacteria and viruses, are increasingly developing resistance to conventional disinfectants. As a result, new approaches to disinfection are being explored, such as the use luminophores that convert visible light into ultraviolet C radiation (UVC). In this work, we present novel UVC phosphors, $A_3Lu(PO_4)_3$ (A = Sr, Ba), activated by Pr^{3+}. These phosphates were synthesized by the Pechini method with different activator concentrations and crystallized in a cubic structure with the space group $I\bar{4}3d$. The emission and excitation spectra, as well as decay times under synchrotron and visible-light excitation, were measured. Both phosphates exhibited efficient and fast 5d−4f emission from 240 to 340 nm, along with a very weak f-f emission line around 600 nm upon ultraviolet excitation. Multiphonon relaxation from the $^3P_0$ to $^1D_2$ state causes the phosphors to emit weak blue ($^3P_1 \rightarrow {}^3H_4$) and intense orange ($^1D_2 \rightarrow {}^3H_4$) light upon direct excitation of the $^3P_2$ level. The upconversion properties of $A_3Lu(PO_4)_3$:Pr^{3+} crystallites were investigated under 444 nm laser excitation, and the effect of Pr^{3+} concentration on these properties was evaluated. Compared to the YPO_4:Pr^{3+} reference material studied earlier, the $Ba_3Lu(PO_4)_3$:Pr^{3+} host showed a 20-fold enhancement in UVC upconversion emission, making this phosphate one of the most efficient visible-to-ultraviolet upconversion matrices to date. Thus, the studied phosphates have potential use in sterilization, disinfection, photocatalysis, and phototherapy.

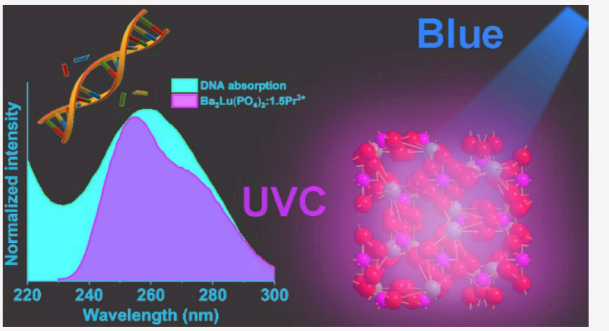

1. INTRODUCTION

Inorganic compounds doped with trivalent lanthanide ions are widely used in various advanced optical and electronic applications due to their sharp emission lines and excellent thermal and chemical stability. Typical applications include phosphors for light-emitting diodes (LED), display technologies, bioimaging and medical diagnostics, anticounterfeiting measures, laser materials, radiation detectors, and dosimeters.[1−4]

Recently, researchers have increasingly focused on a unique process known as upconversion in which multiple low-energy photons are combined to produce a single high-energy photon.[5] This property opens a wide range of applications, especially in biomedical imaging, photodynamic therapy, solar energy harvesting, and disinfection.[6−10] In the latter case, phosphors are being developed that can convert visible light into ultraviolet-C (UV−C) radiation, which has a cytotoxic effect on Deoxyribonucleic Acid (DNA) and ribonucleic acid (RNA), ultimately leading to apoptosis of microorganisms. This development aims to replace mercury lamps with more environmentally friendly and efficient materials. Praseodymium ion (Pr^{3+}) is commonly used as an activator because, depending on the host, it can exhibit efficient photoluminescence in the UV−C range due to the interconfiguration transitions 4f5d → 4f. Ideal matrices for upconversion are compounds in which the $^1S_0$ level of the praseodymium ion is significantly above the lower edge of the 4f5d configuration.[11] Currently, UVC upconversion of Pr^{3+} ions excited by visible light is being studied in various matrices, including fluorides ($RbCaF_3$, $LiYF_4$), phosphates (YPO_4), oxyfluorides ($Y_7O_6O_9$, $Lu_7O_6F_9$, LuOBr), borates (YBO_3) and silicates (Y_2SiO_5, $LiY_9(SiO_4)_6O_2$).[12−19] Due to their simple preparation process, excellent chemical stability, and radiation resistance, phosphates are ideal candidates for upconversion studies.

Furthermore, in our previous work on phosphate upconversion, the praseodymium-activated compound $Ba_3Y(PO_4)_3$ showed a 6-fold increase in upconversion emission compared to the known YPO_4:Pr^{3+}. We decided to build on this success, and in this paper we focus on the upconversion properties of Pr^{3+} -doped eulytite-type orthophosphates $A_3Lu(PO_4)_3$ (A = Sr, Ba). These compounds, doped with rare earth metals such as Ce^{3+}, Eu^{3+}, Sm^{3+}, and Dy^{3+}, have been extensively studied as suitable matrices for various potential optical applications, including displays and LEDs.[20−27] To our knowledge, there is

Received: April 1, 2025
Revised: May 16, 2025
Accepted: May 21, 2025
Published: May 29, 2025

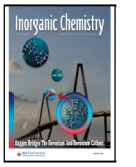

https://doi.org/10.1021/acs.inorgchem.5c01458
Inorg. Chem. 2025, 64, 11146−11154

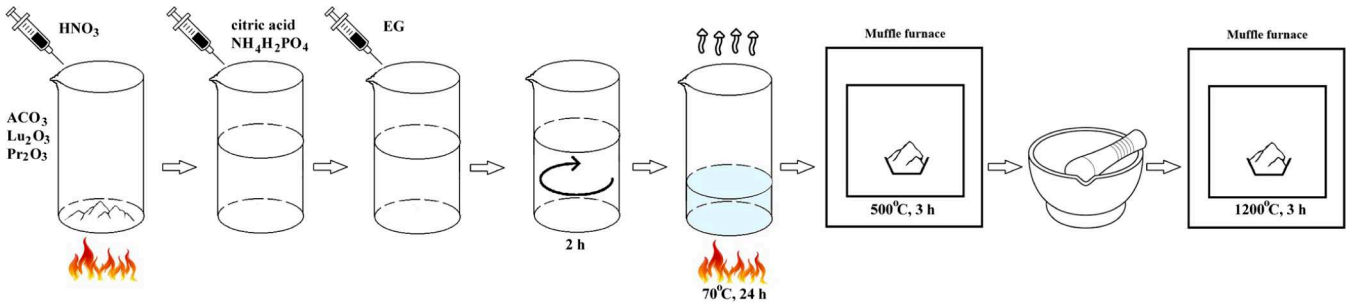

Figure 1. Schematic illustration of the synthesis of $A_3Lu(PO_4)_3:Pr^{3+}$ (A = Sr, Ba) crystallites.

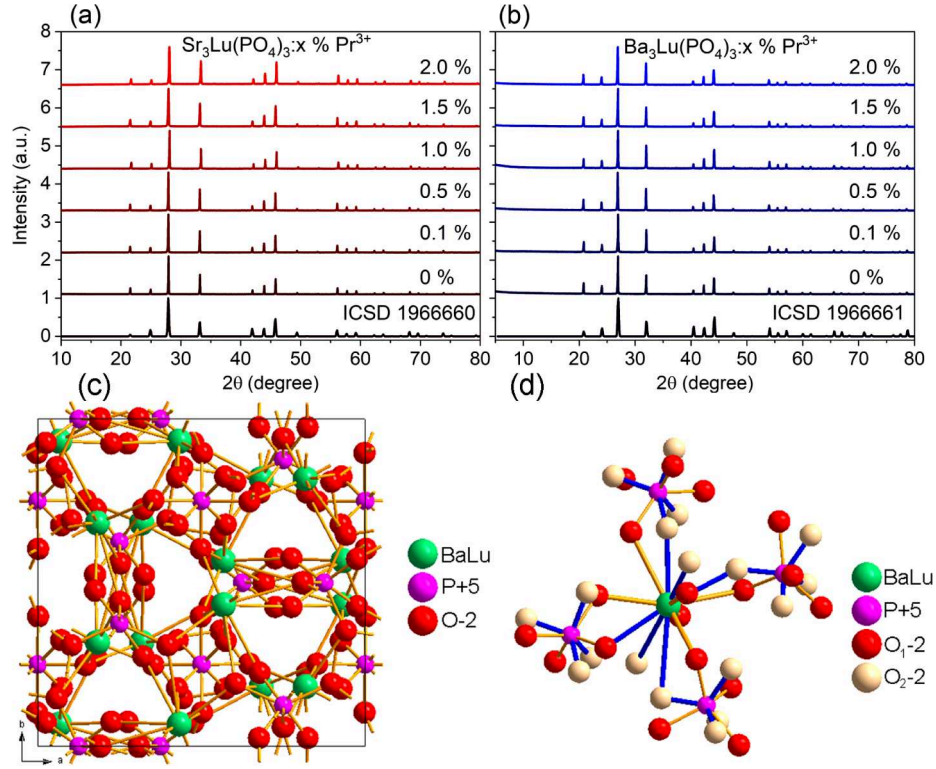

Figure 2. XRPD patterns of $Sr_3Lu(PO_4)_3:Pr^{3+}$ (a) and $Ba_3Lu(PO_4)_3:Pr^{3+}$ (b) phosphors. Crystal structure of $A_3Lu(PO_4)_3$ (A = Sr, Ba) (c) and coordination of A^{2+}/Lu^{3+} cation (d).

currently only one study in the literature on time-resolved vacuum ultraviolet (VUV) spectroscopy of $Ba_3Lu(PO_4)_3:Pr^{3+}$ using synchrotron radiation excitation, and nothing has been reported for strontium-based phosphate.[28] The observed 5d-4f emission of Pr^{3+} ions in the ultraviolet region confirms the potential of $A_3Lu(PO_4)_3$ (A = Sr, Ba) hosts to convert visible light to the UVC region of the spectrum. For the first time, visible luminescence and upconversion properties, including upconversion emission intensity, decay time, and the dependence of emission on pump power, were measured for $A_3Lu(PO_4)_3:Pr^{3+}$ (A = Sr, Ba) crystallites. The study examined the effect of activator concentration on upconversion properties, allowing for the determination of the optimal concentration. When excited by a 444 nm laser, barium-containing phosphate produces ultraviolet emission that is 20 times more intense than that of standard $YPO_4:Pr^{3+}$, making it promising for practical applications.

2. EXPERIMENT

Powder samples of $A_3Lu_{1-x}Pr_x(PO_4)_3$ (A = Sr, Ba) with x = 0, 0.001, 0.005, 0.01, 0.015, and 0.02 were synthesized using the Pechini method. Lutetium oxide (Lu_2O_3; 99.9%), strontium carbonate ($SrCO_3$; 99.9%), barium acetate ($BaCO_3$; 99.9%), ammonium dihydrogen phosphate ($NH_4H_2PO_4$; 99.99%), praseodymium oxide (Pr_2O_3; 99.9%), citric acid ($C_6H_8O_7$, 99.7%) and ethylene glycol (EG, $C_2H_4(OH)_2$, 99%) were used as raw materials without further purification. Stoichiometric amounts of Lu_2O_3, ACO_3, and Pr_2O_3 were dissolved in nitric acid with stirring and heating. To the resulting transparent solution, maintained at room temperature under vigorous stirring, solutions of citric acid, $NH_4H_2PO_4$, and ethylene glycol were added successively. A ratio of citric acid, ethylene glycol and metal cations of 2:2:1 was used. The solution was heated on a hot plate at 80 °C for 24 h to produce a white resin, which was then placed in a crucible. The resin was heat treated in two stages: at 500 °C for 6 h and at 1250 °C for 5 h. Figure 1 schematically shows the stages of the preparation of $A_3Lu(PO_4)_3:Pr^{3+}$ (A = Sr, Ba) crystallites.

https://doi.org/10.1021/acs.inorgchem.5c01458
Inorg. Chem. 2025, 64, 11146−11154

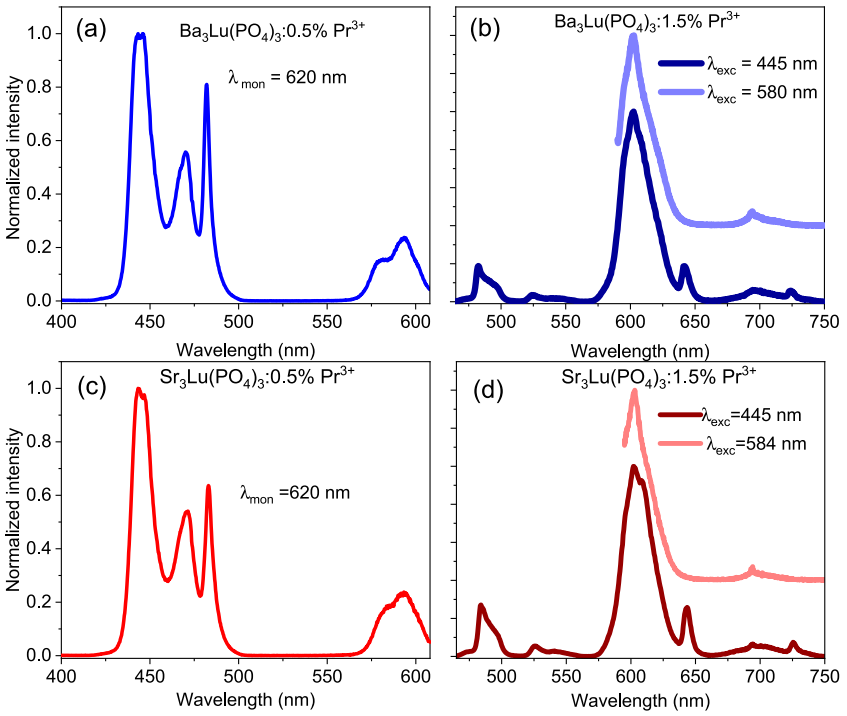

Figure 3. Excitation (a, c) and emission (b, d) spectra of the $A_3Lu(PO_4)_3$:0.5%Pr^{3+} (A = Sr, Ba) phosphors.

The phase purity of the $A_3Lu(PO_4)_3$:Pr^{3+} (A = Sr, Ba) crystallites was checked on an X'Pert PRO X-ray diffractometer with CuKα radiation (λ = 1.54056 Å). The morphology of $A_3Lu(PO_4)_3$:Pr^{3+} (A = Sr, Ba) was examined using a FEI Nova NanoSEM 230 field emission scanning electron microscope (FE-SEM). Images were acquired at 5.0 kV in slow scan mode to enhance resolution and contrast. The powder sample was embedded in carbon resin prior to analysis. Excitation and emission spectra, as well as luminescent decay time, were measured on an FLS1000 fluorescence spectrometer equipped with a 450 W ozone-free xenon lamp and a xenon flash lamp. Upconversion measurements were performed using a VUV McPherson spectrometer equipped with a Hamamatsu R7154P photomultiplier, a UG5 filter (Eksma Optics), and 444 nm continuous-wave laser excitation. To study the upconversion lifetime, the second harmonic of a titanium-sapphire laser, pumped by the second harmonic of a Nd:YAG laser (LOTIS TII Belarus), was used.

The study of excitation and emission spectra, as well as decay kinetics in the ultraviolet range, was conducted at the SUPERLUMI station in DESY (Hamburg, Germany) using a 2-m McPherson monochromator at a synchrotron radiation source. A Hamamatsu R6358 photomultiplier was used as the detector. The excitation spectra were corrected for the incident photon flux of the excitation beam using the excitation spectrum of a reference sodium salicylate sample. The emission spectra were corrected to account for the sensitivity of the detection system.

3. RESULTS AND DISCUSSION

3.1. Synthesis and Characterization of the Structure.

The obtained $Sr_3Lu(PO4)_3$:Pr^{3+} and $Ba_3Lu(PO_4)_3$:Pr^{3+} phosphor powders were assigned to the cubic structure with the space group $I\bar{4}3d$ (Figure 2 a,b). The samples completely crystallized without forming any secondary phases. Although the phosphates were synthesized using the Pechini method, the resulting particles are highly agglomerated, with sizes ranging from a few microns to several tens of microns (Figure S1). Figure 2c,d shows a visualization of the phosphate unit cell and the coordination polyhedra of the A^{2+}/Lu^{3+} cation (A = Ba, Sr). Taking into account the influence of valence, it is assumed that Pr^{3+} more readily replaces Lu^{3+} ions in the crystal lattice compared to divalent alkaline earth metal ions. In the structure, the A^{2+} and Lu^{3+} cations randomly occupy the same C_3 symmetry site, with site occupancies of 0.75 and 0.25, respectively.[29] Since the oxygen atoms are also randomly located at two C_1 sites, there is significant disorder in the crystal lattice, which is reflected in the emission spectra described later in this paper.

3.2. Luminescence Properties in the Visible Range.

Figure 3 a,c shows the excitation spectra of the $A_3Lu(PO_4)_3$:0.5%Pr^{3+} (A = Sr, Ba) phosphors, with measurements taken at 620 nm. Two excitation bands, located in the spectral regions of 425−500 nm and 560−610 nm, correspond to the transition from the ground state of Pr^{3+} ($^3H_4$) to ^3P_J and $^1D_2$, respectively. Since the host lattice is disordered and the Pr^{3+} ions are located in sites that differ in the crystal field strength, the measured excitation bands consist of relatively structureless and significantly broadened bands. This makes these phosphates promising for applications such as the conversion of sunlight to ultraviolet light.

Figure 3b,d shows typical emission spectra of Pr^{3+} ions in phosphate matrices when excited at a wavelength of 445 nm. Since the $^3P_2$, $^3P_1$ and $^3P_0$ levels are very close to each other, the excitation of $^3P_2$ (445 nm) leads to rapid nonradiative relaxation to the $^3P_1$ and $^3P_0$ states. Then, the excited $^3P_0$ state is depopulated into $^1D_2$ via multiphonon relaxation due to the high phonon energy in the phosphate matrices, which is around 1200 cm^{-1}.[30,31] The energy gap between $^3P_0$ and $^1D_2$ levels in the studied phosphates is ~3500 cm^{-1}, and about three phonons are required for relaxation from $^3P_0$ to $^1D_2$.[25] Therefore, the emission from the $^1D_2 \rightarrow {}^3H_4$ transition

https://doi.org/10.1021/acs.inorgchem.5c01458
Inorg. Chem. 2025, 64, 11146−11154

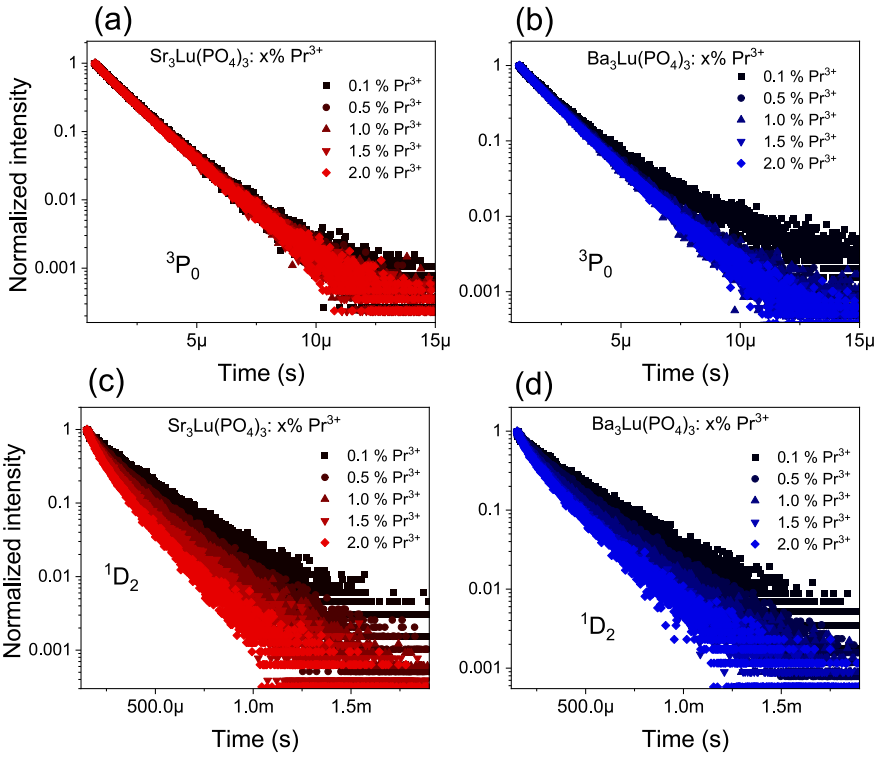

Figure 4. Luminescent decay curves of the $^3P_0$ (a, b) and $^1D_2$ (c, d) emission of the $A_3Lu(PO_4)_3$:Pr^{3+} (A = Sr, Ba) phosphors.

dominates the spectra, while the emission from the $^3P_{1,0}$ to ^3H_J,[3] F_J levels is weak. To confirm that the intense orange luminescence is due to the $^1D_2 \rightarrow {}^3H_4$ transition, the luminescence was studied under direct excitation of the $^1D_2$ level at 580 and 584 nm (Figure 3 b,d).

It should be noted that luminescence under $^3P_0$ excitation strongly depends on the activator concentration. Specifically, as the concentration increases, emission in the 605−610 nm range decreases, likely due to cross-relaxation between neighboring optically active ions. For clarity, the spectra were normalized to the intensity at ∼482 nm ($^3P_0 \rightarrow {}^3H_4$) (Figure S2).

The decay of luminescence of $A_3Lu(PO_4)_3$:Pr^{3+} (A = Sr, Ba) phosphors from the $^3P_0$ and $^1D_2$ states was studied as a function of Pr^{3+} concentration (Figure 4). Since the decay curves of these emissions deviate from an exponential dependence, the luminescent lifetime was determined using the following equation:[32,33]

$$\tau = \frac{\int tI(t)dt}{\int I(t)dt} \quad (1)$$

The integration of the emission intensity was performed for all samples on a scale from 1 to 0. Previously, all minima of the spectra were shifted to zero using the baseline determined for each spectrum separately. The nonexponential luminescence decay kinetics can be related to nonradiative energy transfer processes between excited and unexcited Pr^{3+} ions. Additionally, the variation in the local crystal field surrounding different Pr^{3+} ions causes slight shifts in energy levels and transition rates, leading to a distribution of decay times.[34] The luminescence decay constants are presented in Table 1. Concentration quenching of luminescence causes a decrease in the decay constants with increasing concentration of

Table 1. Luminescent Lifetime for the $^3P_0$ and $^1D_2$ Transition of Pr^{3+} in $A_3Lu(PO_4)_3$ (A = Sr, Ba) Phosphors

	$Sr_3Lu(PO_4)_3$:Pr^{3+}		$Ba_3Lu(PO_4)_3$:Pr^{3+}	
Concentration Pr^{3+}, mol %	$^3P_0$ [μs]	$^1D_2$ [μs]	$^3P_0$ [μs]	$^1D_2$ [μs]
0.1	2.15	375	2.65	408
0.5	2.13	355	2.24	368
1.0	2.10	320	2.21	344
1.5	2.09	294	2.17	319
2.0	2.08	275	2.16	313

praseodymium ions in the samples.[35,36] Typically, in praseodymium-activated matrices, the $^1D_2$ level decays faster with increasing activator concentration in the samples compared to the $^3P_0$ level.[37] This is due to the process of cross-relaxation, which is effective by being allowed by spin. Cross-relaxation occurs in Pr^{3+} ion pairs when the ions are close enough to each other, following the transition [$^1D_2$, $^3H_4$] → [$^1G_4$, $^3F_4$].[38] Cross-relaxation is also effective in depopulating the $^3P_0$ level, but only at room temperature, when the $^3P_0$ is thermally excited through the [$^3P_0$, $^3H_4$] → [$^1D_2$, $^3H_6$] transition. Note that the strontium-based phosphate exhibited a slightly faster luminescence decay constant compared to that of its barium-based counterpart. This is confirmed by the more pronounced cross-relaxation for $Sr_3Lu(PO_4)_3$:Pr^{3+} (Figure S3).

3.3. Luminescence Properties in the Ultraviolet Range. *3.3.1. Stokes Emission.* Using synchrotron radiation, the emission and excitation spectra of Pr^{3+}-doped and undoped matrices were studied at 8 K (Figure 5). The excitation spectra of $Ba_3Lu(PO_4)_3$:0.5% Pr^{3+} and $Sr_3Lu(PO_4)_3$:0.5% Pr^{3+}, monitored at 280 and 275 nm, can be attributed to the $4f^2 \rightarrow 4f^15d^1$ excitation transitions of Pr^{3+}. Figure 5a,c shows the emission spectra of $Ba_3Lu(PO_4)_3$:0.5% Pr^{3+} and $Sr_3Lu(PO_4)_3$:0.5%Pr^{3+} obtained upon excitation of Pr^{3+} $4f^2 \rightarrow$

https://doi.org/10.1021/acs.inorgchem.5c01458
Inorg. Chem. 2025, 64, 11146−11154

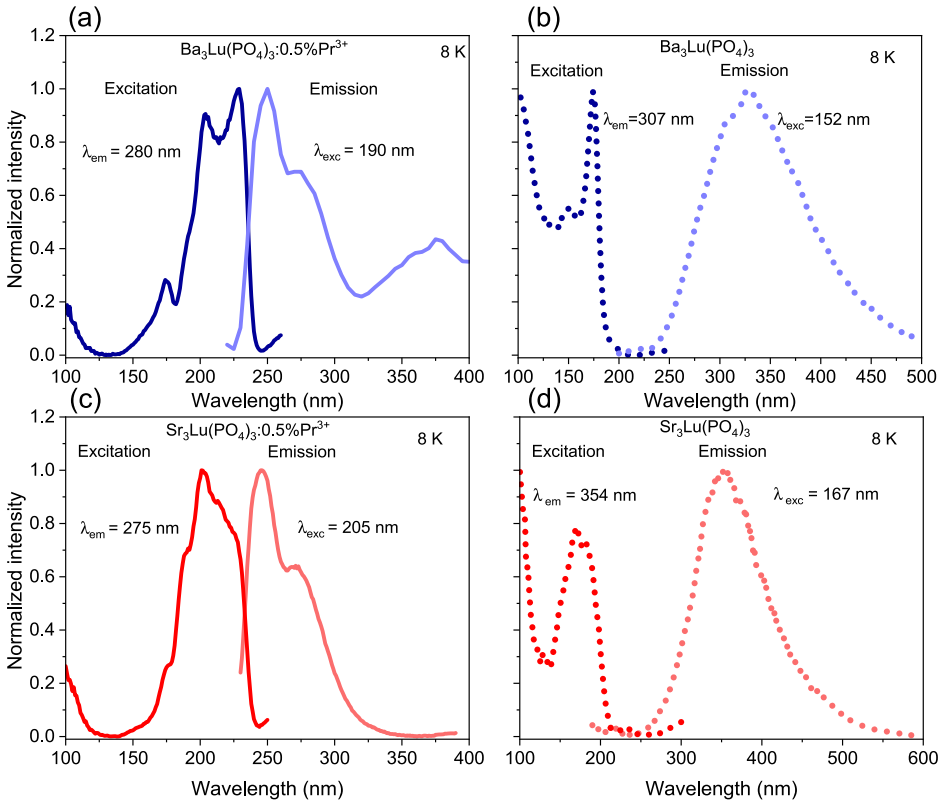

Figure 5. Excitation and emission spectra of $Ba_3Lu(PO_4)_3$:0.5% Pr^{3+} (a), $Ba_3Lu(PO_4)_3$ (b), $Sr_3Lu(PO_4)_3$:0.5% Pr^{3+} (c), and $Sr_3Lu(PO_4)_3$ (d) using synchrotron radiation.

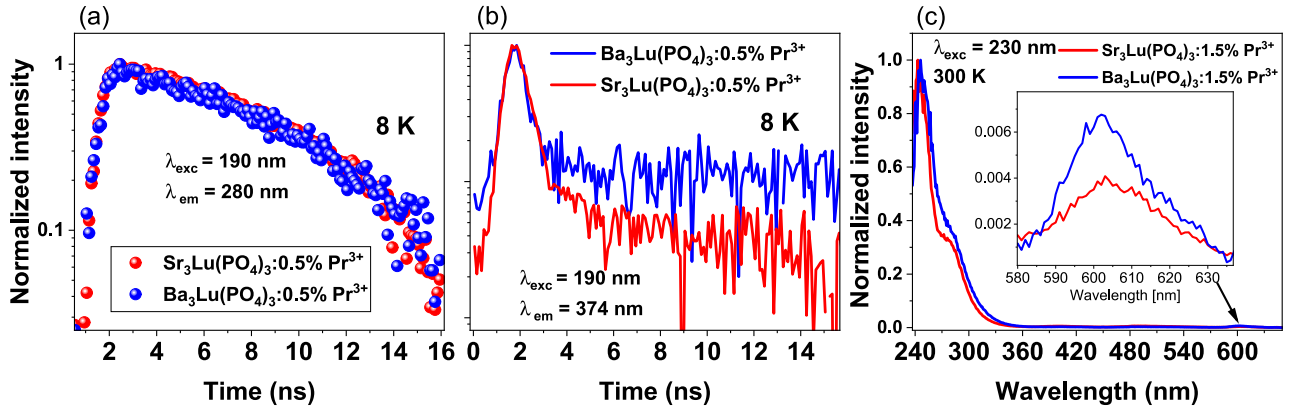

Figure 6. Decay times of $A_3Lu(PO_4)_3$:0.5% Pr^{3+} (A = Sr, Ba) under 190 nm excitation, monitored at 280 nm (a) and 374 nm (b). (c) Room-temperature luminescence spectra of $Sr_3Lu(PO_4)_3$:1.5%Pr^{3+} and $Ba_3Lu(PO_4)_3$:1.5% Pr^{3+} under 230 nm excitation.

$4f^15d^1$ at 190 and 205 nm, respectively. The emission bands detected in the 240 to 340 nm range for both compounds are associated with interconfigurational transitions originating from the lowest excited $4f^15d^1$ state of Pr^{3+} and terminating at the ^3H_J and ^3F_J multiplets of the $4f^2$ ground-state electronic configuration. This is confirmed by the single-exponential behavior of this emission, with an approximate lifetime of $\tau \approx$ 14 ns (Figure 6a). The luminescence spectrum of $Ba_3Lu(PO_4)_3$:0.5% Pr^{3+} exhibits a broad band with a maximum at 374 nm, which is attributed to the emission from its intrinsic defects.[39,40] The lifetime of this emission is 0.5 ns when excited at 190 nm at 8 K (Figure 6b). No impurity luminescence is observed in the emission spectrum of $Sr_3Lu(PO_4)_3$:0.5%Pr^{3+}, as the sample was excited using a wavelength of lower excitation energy (205 nm) compared to the barium-containing compound (190 nm). However, time-resolved emission spectroscopy studies with 190 nm excitation confirm the presence of impurity luminescence characterized by a fast decay constant of 0.4 ns (Figure 6b). Under deep ultraviolet excitation, the emission spectra for both undoped hosts exhibit a broad band ranging from 250 to 500 nm, attributed to intrinsic luminescence caused by self-trapped excitons in pure matrices (Figure 5b,d). Similar emission is also observed in other undoped compounds.[41−43] The excitation spectra of both undoped phosphors correspond to their exciton absorption spectra.[42]

Based on the excitation and emission spectra, the Stokes shift of $Ba_3Lu(PO_4)_3$:0.5% Pr^{3+} is 1463 cm^{-1}, while for $Sr_3Lu(PO_4)_3$:0.5%Pr^{3+} it is 1519 cm^{-1}. The Stokes shift (ΔS) was calculated as the energy difference between the position of

https://doi.org/10.1021/acs.inorgchem.5c01458
Inorg. Chem. 2025, 64, 11146−11154

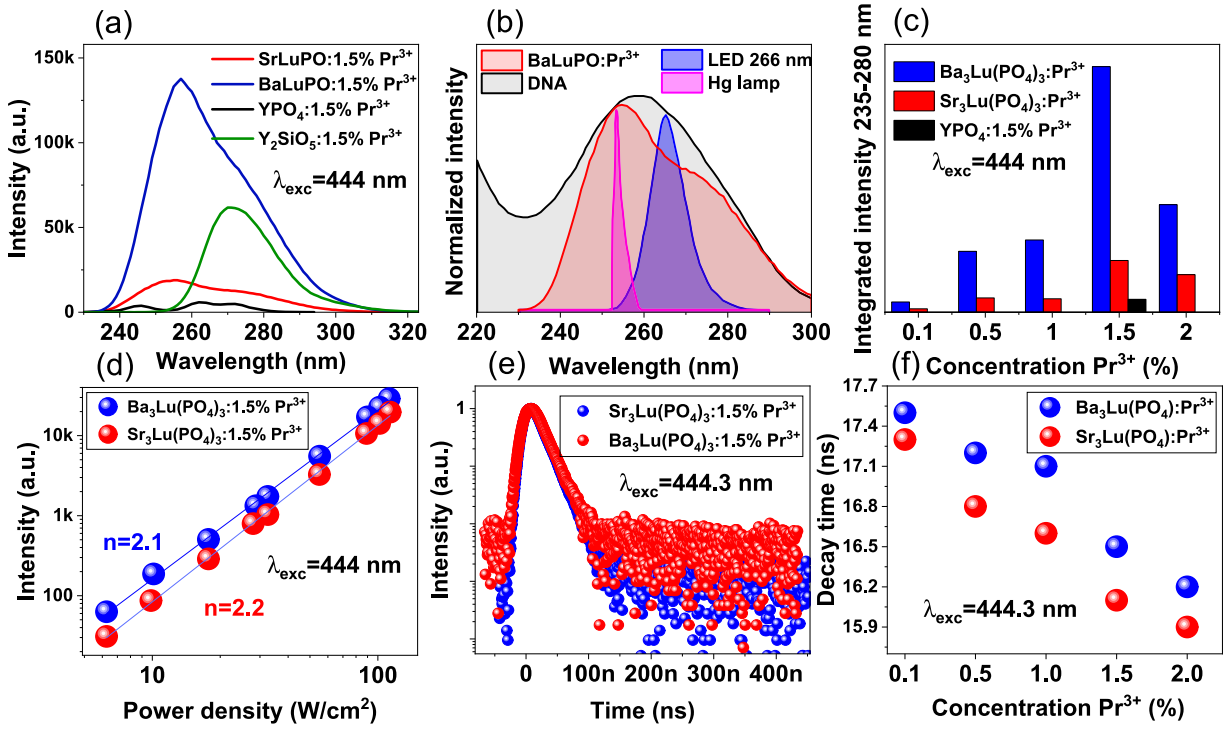

Figure 7. (a) Upconversion emission spectra of $A_3Lu(PO_4)_3$:1.5% Pr^{3+} (A = Sr, Ba), YPO_4:1.5% Pr^{3+}, and Y_2SiO_5:1.5% Pr^{3+} phosphors excited by a 444 nm laser. (b) Normalized typical absorption spectra of DNA, combined with the spectra of UVC LED, mercury (Hg) lamp and upconversion emission $Ba_3Lu(PO_4)_3$:1.5Pr^{3+} under laser excitation 444 nm. (c) Concentration of Pr^{3+} versus integrated upconversion emission intensity in the 235−280 nm range. (d) Dependence of the intensity of upconversion emission on laser pump power for $A_3Lu(PO_4)_3$:1.5% Pr^{3+} phosphor. (e) Decay profiles of the upconverted luminescence of $A_3Lu(PO_4)_3$:1.5%Pr^{3+}. (f) Concentration dependence of decay times for $A_3Lu(PO_4)_3$:Pr^{3+} (A = Sr, Ba).

the lowest energy excitation band and the highest energy emission band (E_{em}).[44] The lowest $4f^15d^1$ energy level for Pr^{3+} (E_{fd}) for crystallites was estimated using the equations:[13]

$$E_{fd} = E_{em} + 1/2\Delta S \quad (2)$$

The lowest $4f^15d^1$ energy level for $Ba_3Lu(PO_4)_3$:0.5% Pr^{3+} is 42,520 cm^{-1}, and for $Sr_3Lu(PO_4)_3$:0.5%Pr^{3+} it is 42,780 cm^{-1}. These values will help later determine which levels of praseodymium are involved in the upconversion process.

Due to the small Stokes shift, the excited 5d electronic configuration depopulates radiatively without feeding the ^3P_J term of the 4f electronic configuration. This is confirmed by the negligible emission in the visible range (Figure 6c). The very weak band around 600 nm is associated with the intraconfigurational $4f^2 \rightarrow 4f^2$ transitions of Pr^{3+} from the $^1D_2$ level to the $^3H_4$ ground state, resulting from nonradiative energy transfer from 5d4f to $4f^2$. The spectra show the absence of $^3P_0$ emission, which is quenched by multiphonon relaxation to the $^1D_2$ multiplet, as observed in the case of $Ca_9Lu(PO_4)_7$:Pr^{3+} and $LaPO_4$:Pr^{3+} phosphates.[44−46]

3.3.2. Anti-Stokes Emission. The upconversion emission spectra of $A_3Lu(PO_4)_3$:1.5% Pr^{3+} (A = Sr, Ba) phosphors excited by a 444 nm laser are shown in Figure 7a. The phosphors emit ultraviolet emission in the range of 235 to 315 nm, with approximately 85% of the total intensity falling in the UVC range and 15% in the UVB range. The integrated upconversion intensity of the studied phosphates in the UVC region was compared with the previously published effective upconverter YPO_4:Pr^{3+}.[17] The studies were carried out under identical conditions, with $Sr_3Lu(PO_4)_3$:1.5% Pr^{3+} showing a 4-fold increase and $Ba_3Lu(PO_4)_3$:1.5% Pr^{3+} a 20-fold increase. Furthermore, the barium-containing phosphate exhibited an almost 4-fold increase in upconversion luminescence in the UVC region compared to Y_2SiO_5:Pr^{3+}. To evaluate the potential applicability of newly synthesized phosphors, the upconversion luminescence spectra were normalized to the absorption spectra of DNA (black line), a mercury lamp (pink line) and the shortest wavelength UV LED currently available (blue line) (Figure 7b).[47−49] The near-complete overlap between the upconversion luminescence and DNA absorption spectrum suggests that DNA may absorb UVC radiation emitted by the phosphor, potentially leading to DNA denaturation.

The relationship between the intensity of upconversion and the Pr^{3+} concentration was also examined (Figure 7c). The emission intensity increased with the Pr^{3+} concentration, achieving optimal performance at 1.5 mol %. In compounds with high phonon energy and efficient energy transfer from the $^3P_0$ to the $^1D_2$ level as a result of multiphonon relaxation, the $^1D_2$ multiplet can act as an intermediate level in the upconversion process.[50,51] Taking the excitation wavelength of 444 nm (22,522 cm^{-1}) and the $^1D_2$ positions for $Ba_3Lu(PO_4)_3$:Pr^{3+} (~17,250 cm^{-1}) and $Sr_3Lu(PO_4)_3$:Pr^{3+} (~17,200 cm^{-1}), the $^1D_2 \rightarrow 4f^15d^1$ transition does not contribute to the upconversion process, since such excitation terminates well below the lower limit of the $4f^15d^1$ band.

To gain a deeper understanding of the upconversion mechanism, the upconversion emission was measured at varying laser pump powers.[52] For a fixed emission wavelength, the upconversion emission intensity (I) versus the laser pump power (P) provides information regarding the number of

https://doi.org/10.1021/acs.inorgchem.5c01458
Inorg. Chem. 2025, 64, 11146−11154

photons (n) contributing to the upconversion luminescence process. This proportionality relationship is given below:[53]

$$I \propto P^n \quad (3)$$

The graphs show a linear dependence of the upconversion emission intensity at a wavelength of 255 nm for $Sr_3Lu(PO_4)_3$:1.5% Pr^{3+} and 256 nm for $Ba_3Lu(PO_4)_3$:1.5% Pr^{3+}, with laser pump powers in the range of 50−850 mW (Figure 7d). The slope values (n) were found to be 2.2 and 2.1, respectively, indicating that a two-photon process is responsible for the upconversion. Two two-photon mechanisms have been proposed in the literature to be responsible for the upconversion of praseodymium ions: energy transfer upconversion (ETU) and excited state absorption (ESA).[1] Since these two processes are difficult to distinguish directly, upconversion lifetimes under pulsed excitation at a wavelength of 444.3 nm were studied to establish the mechanism in the phosphates (Figure 7e). The upconversion decay time constant (τ) was estimated using the equilibrium equation No 1. Since the upconversion lifetime falls within the range of 5d-4f emission decay kinetics, specifically 15.9−17.5 ns, the main mechanism responsible for the upconversion in the studied phosphates is ESA (Figure 7 f).[14] For the ETU mechanism, the upconversion lifetime for our phosphates would be half the time of $^3P_0$, approximately one microsecond (Table 1).

4. CONCLUSIONS

We successfully prepared Pr^{3+}-doped $A_3Lu(PO_4)_3$ crystallites using the Pechini method. Under ultraviolet excitation, the phosphors exhibited an intense and fast emission band in the range of 240−340 nm, attributed to the $4f^15d^1 \rightarrow 4f^2$ interconfigurational transitions of Pr^{3+}, along with a very weak emission line near 600 nm due to nonradiative energy transfer from 5d4f to $4f^2$. $A_3Lu(PO_4)_3$:Pr^{3+} phosphors emit orange light and show anti-Stokes emission in the germicidal region upon direct excitation of the $^3P_2$ level. By examining the relationship between upconversion emission and activator concentration, we identified the optimal activator concentration to be 1.5 mol % for both compounds. Upconversion emission lifetime studies indicated that upconversion occurs as a result of Excited State Absorption. $Ba_3Lu(PO_4)_3$:Pr^{3+} crystallites exhibit highly efficient blue-to-UVC upconversion properties, which makes them attractive for antimicrobial applications. In addition, our research results indicate that the new phosphors exhibit UVC emission when exposed to ultraviolet light.

■ ASSOCIATED CONTENT

Supporting Information

The Supporting Information is available free of charge at https://pubs.acs.org/doi/10.1021/acs.inorgchem.5c01458.

Figures. SEM images of $Sr_3Lu(PO_4)_3$:1.5Pr^{3+} and $Ba_3Lu(PO_4)_3$:1.5Pr^{3+} crystallites. The emission spectra of $Sr_3Lu(PO_4)_3$:xPr^{3+} and $Ba_3Lu(PO_4)_3$:xPr^{3+} crystallites under 445 nm excitation. Integral ratio of the $^3P_0 \rightarrow {}^3H_4$ transition to the $^1D_2 \rightarrow {}^3H_4$ transition (PDF)

■ AUTHOR INFORMATION

Corresponding Author

Nadiia Rebrova − *Institute of Low Temperature and Structure Research, Polish Academy of Science, Wrocław 50-422, Poland;* orcid.org/0000-0002-7536-2642; Email: n.rebrova@intibs.pl

Authors

Alexander Grippa − *Institute for Scintillation Materials, National Academy of Sciences of Ukraine, Kharkiv 61001, Ukraine;* orcid.org/0000-0002-2429-2955

Patrycja Zdeb-Stańczykowska − *Institute of Low Temperature and Structure Research, Polish Academy of Science, Wrocław 50-422, Poland;* orcid.org/0009-0008-6368-4784

Przemysław J. Dereń − *Institute of Low Temperature and Structure Research, Polish Academy of Science, Wrocław 50-422, Poland;* orcid.org/0000-0001-6316-6954

Complete contact information is available at: https://pubs.acs.org/10.1021/acs.inorgchem.5c01458

Author Contributions

N.R.: synthesis, investigation, analysis, data curation, writing original draft, conceptualization; A.G.: investigation, analysis, data curation, writing original draft, conceptualization; P.Z.-S.: investigation, data curation; P.J.D.: conceptualization, methodology, supervision, funding acquisition, writing original draft, project administration. All authors have approved the final version of the manuscript.

Notes

The authors declare no competing financial interest.

■ ACKNOWLEDGMENTS

This work was supported by the National Science Centre under Grant No. UMO-2021/41/B/ST5/03792, which is gratefully acknowledged. The investigation using synchrotron radiation at the P66 SUPERLUMI station at DESY, Hamburg, Germany, was performed within the framework of the I-20240194 EC project. One of the authors, A. Grippa (Oleksandr Gryppa), is thankful to the Polish Academy of Sciences for its support through the PAN-NANU (PAS-NASU) program for scientists cooperating with INTiBS PAN.

■ REFERENCES

(1) Dhale, S. P.; Ugemuge, N. S.; Singh, V.; Moharil, S. V. Na_2MgAlF_7: Ln^{3+} (Ln^{3+} = Ce, Gd) Weberite Downshifting Phosphor for Designing UVB LED. *J. Mater. Sci.* **2024**, *59* (34), 16158−16169.

(2) Dhale, S. P.; Ugemuge, N. S.; Singh, V. S.; Nagpure, I. M.; Nafdey, R. A.; Moharil, S. V. Synthesis and Spectroscopic Analysis of $NaCaYF_6$: Nd^{3+}, Yb^{3+}NIR Emitting Phosphor. *J. Mol. Struct.* **2025**, *1323*, 140588.

(3) Kshetrapal, S.; Ugemuge, N.; Dhale, S.; Nafdey, R.; Moharil, S. V. Photoluminescence in Eulytite-Type Structure $Ca_3Bi(PO_4)_3$: Nd^{3+}/Yb^{3+} Phosphors for Near-Infrared Applications. *J. Electron. Mater.* **2025**, *54* (3), 2275−2286.

(4) Kshetrapal, S.; Ugemuge, N.; Ahamad, H. S.; Nafdey, R.; Moharil, S. V. Spectroscopic Analysis of Nd^{3+}doped $Ba_3Bi(PO_4)_3$ Phosphor for near-Infrared Laser Application. *J. Mol. Struct.* **2025**, *1322*, 140336.

(5) Auzel, F. Upconversion and Anti-Stokes Processes with f and d Ions in Solids. *Chem. Rev.* **2004**, *104* (1), 139−174.

(6) Song, N.; Fan, X.; Guo, X.; Tang, J.; Li, H.; Tao, R.; Li, F.; Li, J.; Yang, D.; Yao, C.; Liu, P. A DNA/Upconversion Nanoparticle Complex Enables Controlled Co-Delivery of CRISPR-Cas9 and Photodynamic Agents for Synergistic Cancer Therapy. *Adv. Mater.* **2024**, *36* (15), 2309534.

(7) Ghazy, A.; Safdar, M.; Lastusaari, M.; Savin, H.; Karppinen, M. Advances in Upconversion Enhanced Solar Cell Performance. *Sol. Energy Mater. Sol. Cells* **2021**, *230*, 111234.

(8) Ekim, U.; Özkutay, D.; Çelikbilek Ersundu, M.; Ersundu, A. E. Full-Color Dynamic Volumetric Displays with Tunable Upconversion Emission from RE^{3+}-Doped Glasses (RE = Ho, Tm, Nd, Yb) under NIR Laser Excitation. *Light: Sci. Appl.* **2025**, *14* (1), 15.
(9) Gao, D.; Chen, B.; Sha, X.; Zhang, Y.; Chen, X.; Wang, L.; Zhang, X.; Zhang, J.; Cao, Y.; Wang, Y.; Li, L.; Li, X.; Xu, S.; Yu, H.; Cheng, L. Near Infrared Emissions from Both High Efficient Quantum Cutting (173%) and Nearly-Pure-Color Upconversion in $NaY(WO_4)_2$: Er^{3+}/Yb^{3+} with Thermal Management Capability for Silicon-Based Solar Cells. *Light: Sci. Appl.* **2024**, *13* (1), 17.
(10) Du, Y.; Jin, Z.; Li, Z.; Sun, T.; Meng, H.; Jiang, X.; Wang, Y.; Peng, D.; Li, J.; Wang, A.; Zou, H.; Rao, F.; Wang, F.; Chen, X. Tuning the 5d State of Pr^{3+} in Oxyhalides for Efficient Deep Ultraviolet Upconversion. *Adv. Opt. Mater.* **2024**, *12* (30), 2400971.
(11) Dramićanin, M. D.; Brik, M. G.; Antić, Ž.; Bănică, R.; Mosoarca, C.; Dramićanin, T.; Ristić, Z.; Dima, G. D.; Förster, T.; Suta, M. Pr^{3+} Visible to Ultraviolet Upconversion for Antimicrobial Applications. *Nanomater. Multidisciplinary Digital Publishing Institute (MDPI)* **2025**, *15*, 562.
(12) Zhao, X.; Liu, F.; Shi, T.; Wu, H.; Zhang, L.; Zhang, J.; Wang, X.; Liu, Y. Conceptual Ultraviolet-C Light Source Based on Up-Conversion Luminescence. *Adv. Photonics Res.* **2022**, *3* (9), 2200106.
(13) Rebrova, N.; Zdeb, P.; Dereń, P. J. Synthesis and Upconversion Luminescence of $LiY_9(SiO_4)_6O_2$ Phosphor Doped with Pr^{3+}. *J. Phys. Chem. C* **2024**, *128* (22), 9090−9098.
(14) Lai, F.; Xu, X.; Shen, J.; Wang, Y.; Yan, Y.; Nie, Y.; You, W.; Wu, D.; Han, L.; Xiao, Z. Structure and Upconversion Luminescence Properties of Pr^{3+}-Doped Y_2SiO_5 Phosphor. *Silicon* **2023**, *15* (4), 1913−1923.
(15) Sun, Y.; Wang, Y.; Hu, C.; Zhou, X.; Hao, J.; Li, W.; Li, H. Energy Transfer from Pr^{3+} to Gd^{3+} and Upconversion Photoluminescence Properties of $Y_7O_6F_9$: Pr^{3+}, Gd^{3+}. *Materials* **2022**, *15* (21), 7680.
(16) Du, Y.; Jin, Z.; Li, Z.; Sun, T.; Meng, H.; Jiang, X.; Wang, Y.; Peng, D.; Li, J.; Wang, A.; Zou, H.; Rao, F.; Wang, F.; Chen, X. Tuning the 5d State of Pr^{3+} in Oxyhalides for Efficient Deep Ultraviolet Upconversion. *Adv. Opt. Mater.* **2024**, *12*, 2400971.
(17) Zhu, Z.; Wang, Y.; Zhang, W.; Wu, T.; Wang, X.; Yang, Y.; Wang, T.; Xu, X. Ultraviolet C Random Lasing at 230−280 Nm from Pr^{3+} Doped Bulk Crystal Resonators by Two-Photon Absorption. *Opt. Lett.* **2022**, *47* (7), 1879.
(18) Wu, J.; Zheng, H.; Liu, X.; Han, B.; Wei, J.; Yang, Y. UVC Upconversion Material under Sunlight Excitation: $LiYF_4$: Pr^{3+}. *Opt. Lett.* **2016**, *41* (4), 792.
(19) Rebrova, N.; Grippa, A.; Zdeb, P.; Dereń, P. J. Blue to UV Upconversion Properties of Pr^{3+} Doped $ACaF_3$ (A = K, Rb, Cs) Phosphors. *Scr. Mater.* **2025**, *255*, 116395.
(20) Wang, T.; Hu, Y.; Chen, L.; Wang, X.; He, M. An Intense Single-Component Warm-White-Light $Sr_3Lu(PO_4)_3$: Dy^{3+} Phosphor for White UV-LEDs. *J. Mater. Sci.: Mater. Electron.* **2016**, *27* (12), 13235−13241.
(21) Xie, M.; Ruan, W.; Wang, J. Energy Transfer, Tunable Photoluminescence of $Sr_3Lu(PO_4)_3$: Tb^{3+}, Eu^{3+} Phosphors. *J. Lumin.* **2020**, *224*, 117278.
(22) Guo, N.; Zheng, Y.; Jia, Y.; Qiao, H.; You, H. Warm-White-Emitting from Eu2+/Mn2+-Codoped $Sr_3Lu(PO_4)_3$ Phosphor with Tunable Color Tone and Correlated Color Temperature. *J. Phys. Chem. C* **2012**, *116* (1), 1329−1334.
(23) Du, J.; Xu, D.; Gao, X.; Yang, Z.; Sun, J. A Novel Orange-Red Emitting Phosphor $Sr_3Lu(PO_4)_3$: Sm^{3+} for near UV-Pumped White Light-Emitting Diodes. *J. Mater. Sci.: Mater. Electron.* **2017**, *28* (11), 8136−8143.
(24) Yang, Z.; Xu, D.; Sun, J. Synthesis and Luminescence Properties of $Ba_3Lu(PO_4)_3$: Sm^{3+} Phosphor. In *Light, Energy and the Environment; OSA Technical Digest (online)*; Optica Publishing Group: Leipzig, 2016.
(25) Jin, C.; Ma, H.; Liu, Y.; Liu, Q.; Dong, G.; Yu, Q. Tunable Luminescence Properties and Energy Transfer in $Ba_3Lu(PO_4)_3$: Ce^{3+},Tb^{3+} Phosphors. *J. Alloys Compd.* **2014**, *613*, 275−279.
(26) Guo, N.; Huang, Y.; Jia, Y.; Lv, W.; Zhao, Q.; Lü, W.; Xia, Z.; You, H. A Novel Orange-Yellow-Emitting $Ba_3Lu(PO_4)_3$: Eu^{2+},Mn^{2+} Phosphor with Energy Transfer for UV-Excited White LEDs. *Dalton Trans.* **2013**, *42* (4), 941−947.
(27) Wang, T.; Hu, Y.; Chen, L.; Wang, X.; He, M. An Intense Red-Emitting Phosphor $Sr_3Lu(PO_4)_3$: Eu^{3+} for near Ultraviolet Light Emitting Diodes Application. *Ceram. Int.* **2016**, *42* (2, Part B), 3659−3665.
(28) Ivanovskikh, K.; Meijerink, A.; Ronda, C.; Piccinelli, F.; Speghini, A.; Bettinelli, M. Fast UV Luminescence in Pr^{3+}-Doped Eulytite Double Phosphates. *Opt. Mater.* **2011**, *34* (2), 419−423.
(29) Wang, Z.; Xia, Z.; Molokeev, M. S.; Atuchin, V. V.; Liu, Q. Blue-Shift of Eu2+ Emission in $(Ba,Sr)_3Lu(PO_4)_3$: Eu^{2+} Eulytite Solid-Solution Phosphors Resulting from Release of Neighbouring-Cation-Induced Stress. *Dalton Trans.* **2014**, *43* (44), 16800−16804.
(30) Gao, G.; Turshatov, A.; Howard, I. A.; Busko, D.; Joseph, R.; Hudry, D.; Richards, B. S. Up-Conversion Fluorescent Labels for Plastic Recycling: A Review. *Adv. Sustain. Syst.* **2017**, *1* (5), 1600033.
(31) Weber, M. J. Multiphonon Relaxation of Rare-Earth Ious in Yttrium Orthoaluminate. *Phys. Rev. B* **1973**, *8*, 54.
(32) Sha, X.; Chen, X.; Gao, D.; Zhang, Y.; Wang, L.; Zhang, Y.; Liu, T.; Zhang, J.; Zhang, X.; Cao, Y.; Wang, Y.; Li, L.; Xu, S.; Li, X.; Yu, H.; Hua, R.; Chen, B. Continuous Tuning of Optical Transition Properties and Phonon Spectrum in Er^{3+} Doped Germano-Tellurite Glass System. *J. Lumin.* **2024**, *275*, 120746.
(33) Zatryb, G.; Klak, M. M. On the Choice of Proper Average Lifetime Formula for an Ensemble of Emitters Showing Non-Single Exponential Photoluminescence Decay. *J. Phys.: Condens. Matter* **2020**, *32* (41), No. 415902.
(34) Tkachuk, A. M.; Ivanova, S. E.; Mirzaeva, A. A.; Joubert, M.-F.; Guyot, Y.; Mirzaeva, A. A.; Joubert, M.-F. Spectroscopic Characteristics of Pr-Doped $Na_{0.4}Y_{0.6}F_{2.2}$ Crystals, Promising for Lasing in near IR and Visible Range Spectroscopic Characteristics of Pr-Doped N AOA $Y_{O.6}F_{2.2}$. In *Crystals, Promising for Lasing in near IR and Visible Range*; IEEE. 2014.
(35) Dereń, P. J.; Mahiou, R.; Goldner, P. Multiphonon Transitions in $LaAlO_3$ Doped with Rare Earth Ions. *Opt. Mater.* **2009**, *31* (3), 465−469.
(36) Dereń, P. J. Spectroscopic Characterization of $LaALO_3$ Crystal Doped with Pr^{3+} Ions. *J. Lumin.* **2007**, *122*−*123*, 40−43.
(37) Kaczkan, M.; Boruc, Z.; Fetlinski, B.; Turczynski, S.; Malinowski, M. Temperature Dependence of $^3P_0$ Pr^{3+} Fluorescence Dynamics in Y4Al2O9 Crystals. *Appl. Phys. B: Lasers Opt.* **2013**, *113* (2), 277−283.
(38) Zdeb, P.; Rebrova, N.; Lisiecki, R.; Dereń, P. J. Luminescence Properties of an Orthorhombic $KLaF_4$ Phosphor Doped with Pr^{3+} Ions under Vacuum Ultraviolet and Visible Excitation. *Materials* **2024**, *17*, 6.
(39) Ma, C. G.; Trevisani, M.; Piccinelli, F.; Ivanovskikh, K. V.; Bettinelli, M.; Brik, M. G. Analysis of Vacuum Ultraviolet Electronic Spectra of Ce^{3+} and Pr^{3+} Ions in $Ca_9Lu(PO_4)_7$: Crystal-Field Calculations and Simulation of Optical Spectra. *J. Phys.: Condens. Matter* **2013**, *25*, 16.
(40) Trevisani, M.; Ivanovskikh, K. V.; Piccinelli, F.; Speghini, A.; Bettinelli, M. Interconfigurational 5d → 4f luminescence of Ce3+ and Pr3+ in Ca9Lu(PO4)7. *J. Phys.: Condens. Matter* **2012**, *24* (38), 385502.
(41) Shalapska, T.; Stryganyuk, G.; Gektin, A.; Demchenko, P.; Voloshinovskii, A.; Dorenbos, P. Crystal Structure and Luminescence Properties of $LiYP_4O_{12}$: Ce^{3+} Phosphor. *J. Phys.: Condens. Matter* **2010**, *22* (48), 485503.
(42) Rebrova, N.; Lisiecki, R.; Zdeb-Stańczykowska, P.; Zorenko, Y.; Voloshinovskii, A.; Pushak, A.; Dereń, P. J. Optical and Upconversion Properties of $A_3Y(PO_4)_3$: Pr^{3+} (A = Sr, Ba) Phosphors. *J. Phys. Chem. C* **2025**, *129* (3), 1873−1884.
(43) Ivanovskikh, K. V.; Meijerink, A.; Piccinelli, F.; Speghini, A.; Zinin, E. I.; Ronda, C.; Bettinelli, M. Optical Spectroscopy of $Ca_3Sc_2Si_3O_{12}$, $Ca_3Y_2Si_3O_{12}$ and $Ca_3Lu_2Si_3O_{12}$ Doped with Pr^{3+}. *J. Lumin.* **2010**, *130* (5), 893−901.

https://doi.org/10.1021/acs.inorgchem.5c01458
Inorg. Chem. 2025, 64, 11146−11154

(44) Srivastava, A. M.; Setlur, A. A.; Comanzo, H. A.; Beers, W. W.; Happek, U.; Schmidt, P. The Influence of the Pr^{3+} 4f15d1 Configuration on the $^1S_0$ Emission Efficiency and Lifetime in $LaPO_4$. *Opt. Mater.* **2011**, *33* (3), 292−298.
(45) Watras, A.; Carrasco, I.; Pazik, R.; Wiglusz, R. J.; Piccinelli, F.; Bettinelli, M.; Deren, P. J. Structural and Spectroscopic Features of $Ca_9M(PO_4)_7$ (M = Al^{3+}, Lu^{3+}) Whitlockites Doped with Pr^{3+} Ions. *J. Alloys Compd.* **2016**, *672*, 45−51.
(46) Srivastava, A. M.; Jennings, M.; Collins, J. The Interconfigurational ($4f^1d^1 \rightarrow 4f^2$) Luminescence of Pr^{3+}in $LuPO_4$, $K_3Lu(PO_4)_2$ and $LiLuSiO_4$. *Opt. Mater.* **2012**, *34* (8), 1347−1352.
(47) Bhardwaj, S. K.; Singh, H.; Deep, A.; Khatri, M.; Bhaumik, J.; Kim, K. H.; Bhardwaj, N. UVC-Based Photoinactivation as an Efficient Tool to Control the Transmission of Coronaviruses. *Sci. Total Environ.* **2021**, *792*, 148548.
(48) Pizzichetti, R.; Martín-Gamboa, M.; Pablos, C.; Reynolds, K.; Stanley, S.; Dufour, J.; Marugán, J. Environmental Life Cycle Assessment of UV-C LEDs vs. Mercury Lamps and Oxidant Selection for Diclofenac Degradation. *Sustainable Mater. Technol.* **2024**, *41*, No. e01002.
(49) Song, C.; Wen, R.; Zhou, J.; Zeng, X.; Kou, Z.; Li, Y.; Yun, F.; Wu, R. UV C Light from a Light-Emitting Diode at 275 Nanometers Shortens Wound Healing Time in Bacterium- and Fungus-Infected Skin in Mice. *Microbiol. Spectrum.* **2022**, *10* (6), No. e0342422.
(50) Cates, E. L.; Li, F. Balancing Intermediate State Decay Rates for Efficient Pr^{3+} Visible-to-UVC Upconversion: The Case of β-$Y_2Si_2O_7$:Pr^{3+}. *RSC Adv.* **2016**, *6* (27), 22791−22796.
(51) Zdeb, P.; Rebrova, N.; Dereń, P. J. Discovering the Potential of High Phonon Energy Hosts in the Field of Visible-to-Ultraviolet C Upconversion. *J. Phys. Chem. Lett.* **2024**, *15* (37), 9356−9360.
(52) Rebrova, N. Luminescence and Upconversion Properties of Pr^{3+}-Doped $CsSrF_3$ Fluoroperovskite. *J. Lumin.* **2025**, *281*, 121190.
(53) Rebrova, N.; Zdeb, P.; Lemański, K.; Macalik, B.; Bezkrovnyi, O.; Dereń, P. J. Upconversion Luminescence Properties of Pr^{3+}-Doped $BaYF_5$ Nanoparticles Prepared by Microwave Hydrothermal Method. *Inorg. Chem.* **2024**, *63* (6), 3028−3036.

https://doi.org/10.1021/acs.inorgchem.5c01458
Inorg. Chem. 2025, 64, 11146−11154